IEEE Access
Multidisciplinary ⋮ Rapid Review ⋮ Open Access Journal

Received 12 April 2024, accepted 2 May 2024, date of publication 13 May 2024, date of current version 24 May 2024.

Digital Object Identifier 10.1109/ACCESS.2024.3399829

RESEARCH ARTICLE

Design and Performance Evaluation of a Low-Cost Non-Invasive Electromechanical Ventilator With Feedback Mechanism

NUZAT NUARY ALAM, RETHWAN FAIZ, MD. SAYZAR RAHMAN AKASH, TANVER SHIDDIQUE, FAIRUZA FAIZ, AND MOHAMMAD HASAN IMAM, (Member, IEEE)
Department of Electrical and Electronic Engineering, American International University-Bangladesh (AIUB), Dhaka 1229, Bangladesh

Corresponding author: Mohammad Hasan Imam (hasan.imam@aiub.edu)

This research was conducted at the Faculty of Engineering under the Centre for Biomedical Research (CBR), Dr. Anwarul Abedin Institute of Innovation in American International University-Bangladesh.

This work involved human subjects or animals in its research. Approval of all ethical and experimental procedures and protocols was granted by the Ethical Review board, American International University-Bangladesh and performed in line with the Declaration of Helsinki.

ABSTRACT Non-invasive ventilators (NIV) are widely utilized in managing both acute and chronic respiratory failure. Operating by delivering oxygenated air into the lungs through positive air pressure, they demand vigilant supervision and adjustment to prevent complications. Key challenges in NIV advancement include enhancing patient-device synchrony, monitoring capabilities, portability, affordability, and user-friendly operation with diverse modes to improve patient adherence. This study introduces an innovative non-invasive electromechanical ventilator that autonomously adjusts based on two types of real-time biofeedback data, providing respiratory support to individual patient needs. The system monitors two vital biofeedback signals—oxygen saturation (SpO2) and respiratory rate (RR)—to determine the optimal breathing mode and ceases operation once the patient's vitals reach a safe range. To acquire biofeedback parameters, a MATLAB simulation model incorporating discrete wavelet transform was designed to extract RR from real-time photoplethysmography (PPG) signals. Comparing hardware-generated results with the simulation outputs yields a mean absolute percentage error (MAPE) of under 10%. Further analyses using Box-whisker and Bland-Altman methods demonstrate significant agreement between measured and simulated RR, particularly among younger demographics. This ventilator system achieves an average accuracy of more than 80% in delivering appropriate breathing patterns based on patient biofeedback. Designed for both home and clinic use, this portable ventilator provides relief from respiratory distress with an intuitive control interface that requires minimal medical expertise.

INDEX TERMS Breathing aid, continuous positive airway pressure, different ventilation modes, discrete wavelet transforms, feedback mechanism, non-invasive ventilator, photoplethysmography signal, respiratory rate (RR), SpO_2.

I. INTRODUCTION

During COVID-19, the use of NIV outside the ICU was found feasible and the overall rate of success was approximately 65% [1], since then it has prompted research on development of open source and low-cost NIV for emergency deployment to combat global ventilator shortage. NIV is used as an initial emergency response for the treatment of patients suffering from moderate to severe acute respiratory failure and mostly remains as an ad-hoc solution to invasive ventilation in emergencies. But during pandemic the efficacy of NIV suppressed the invasive mechanical ventilation (IMV) due to patient's resistance to intubation and higher mortality rate with IMV which has been reported by Menzella et al. [2] and

The associate editor coordinating the review of this manuscript and approving it for publication was Wenbing Zhao.

Mukhtar et al. [3] respectively. Literature likewise supports the efficacy of NIV which are equipped with state of art sensors and microcontrollers hence has led a growing demand for home and portable ventilators. Most of the published works have proposed either a form of conventional bag valve mask (BVM) [4] or a pressure regulatory valve system [5]. A BVM system integrates electronic bag squeezing mechanism at a set frequency [6], [7], [8], [9] based on an idea first reported in a research paper by Husseini et al. [10]. One of the main disadvantages of these type of systems is that the air volume cannot be adjusted based on the patient's requirement which thus poses a potential risk of damage to the lungs [11], [12]. In more recent BVM models researchers have addressed this problem by incorporating advanced electronics and mechanics. AmboVent [13] is the BVM type ventilator, which is instrumented with a valve, a positive end expiratory pressure (PEEP) adapter, a reservoir bag, a heat-moisture exchanger (HME) filter to control breathing speed, maximum peak pressure and volume during an emergency. A cost-efficient ventilation machine was proposed by Shahid et al. [14] which demonstrate the mechanism of an artificial manual breathing unit (AMBU) which was equipped with pressure sensor, microcontroller, breath analyzer (e.g. CO_2 sensor) integrated with cam shaft and chained plank mechanism for operation. However, more recent models have incorporated an electric blower [10], [15], [16], air pump [17], high-pressure turbine [18], [19] in their designs to replace the traditional BVM and effectively demonstrated the reduction in the chances of lung injury from ventilation operation.

The key features of these systems include monitoring various ventilator related parameters such as delivered air volume, Breaths Per Minute (BPM), inspiration to expiration ratio and PEEP rate. Additionally, these systems incorporate multiple modes of ventilation for classified patients such as adults, children and infants. Reports have shown these non-invasive devices to have low fabrication cost approximately in the order of $75 to $200 [10], [11], [12]. However, these economic, non-invasive continuous positive airway pressure (CPAP) ventilators lack the capability to adjust the ventilatory parameters automatically based on the breathing requirement of the patients hence unable to ensure lung protective ventilation. Additionally, such ventilators are not a suitable support for recovery where the patients can be put on NIV for further treatment. Deep learning models have now been used to measure the efficacy of NIV in post critical care after extubating [20]. Collaboration with lung diseases detection deep learning models [21] can bring significant improvement in the NIV control and natural ventilation.

Recent research efforts have tried to understand essential ventilatory parameters such as inspiratory time, RR, tidal volume, percentage oxygen (FiO_2) and adjustable PEEP for a more appropriate ventilator system design and function [22], [23], [24]. According to several studies [25], [26] a poor NIV tolerance is associated with asynchronies between ventilator and patient. Also, it has been demonstrated that increasing the degree of synchrony can improve the patient's comfort during NIV [27]. In the light of this, Hansen et al. [28] proposed the O2matic®-based closed-loop controlled oxygen supply system for home user which controls oxygen supply based on patient's SpO_2 level, but it comes with the limitation of flow rate which it adjusts based on 15s average of saturation readings. Moreover, the cost of this device is £5,000 to £7,000 per unit [29] which is substantially higher for the people of underdeveloped or developing countries.

Considering the existing limitations in developing a reliable, low cost and safe design for the NIV, the current study aims to contribute towards an improved performance by proposing a bio feedback mechanism by incorporating the measurement of two bio signals simultaneously to control ventilation pattern. Additionally, the system autonomously reads vital signs and adjusts ventilation control parameters without requiring any direct involvement from the patient or medical staff. It also aims to terminate the gas flow automatically without any human intervention when the patient's body vitals reach the normal level and as a result it is capable to save oxygen. A key attribute of the suggested system is its minimal need for prior medical expertise, making it user-friendly for individuals at home as a straightforward plug-and-play device. This work offers a physical method to quantitatively measure the efficiency of the proposed system by designing a working prototype which is an extension of the study by Faiz et al. [30]. Lastly, this study aims to develop an easy-to-build, portable, cost-effective and automatic non-invasive bio-feedback mechanism-based ventilator for emergency use in home care and non-critical hospital scenarios as a standalone CPAP device for management of chronic obstructive pulmonary disease (COPD) and acute respiratory distress syndrome (ARDS).

In this paper, a comprehensive investigation into the development of a non-invasive ventilator with feedback mechanism has been presented. To facilitate clarity and ease of understanding, the paper is organized into four main sections: proposed methodology (Section II) describes the framework of the proposed method including feedback system operation and its block diagrams, implementation of hardware and associated challenges (Section III), results and discussion (Section IV) with existing limitations and future directions, and conclusion (Section V). Each section contributes essential insights into various phases of proposed ventilator advancement, allowing readers to follow the logical progression of this study.

II. PRPOSED METHODOLOGY

The basic concept of the proposed model is shown in Fig.1. The designed ventilator box intervenes between medical oxygen cylinder and patient's nasal canula or face mask. The incorporation of biofeedback in this design ensures oxygen flow control via SpO_2 and allows the system to stop when the patient's oxygen saturation reaches optimum condition. The feedback mechanism offers provision for adjustment of

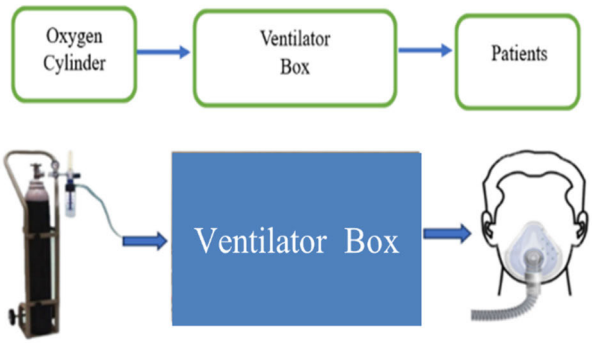

FIGURE 1. Basic blocks of the proposed model.

ventilatory parameters such as I:E ratio based on patient's respiratory rate and oxygen saturation level to minimize the propensity of induced lung injury among patient groups, who are likely to take spontaneous breath. Thus, this design aims to facilitate non-critical patients at home by bringing effective technology to the bedside to assist with breathing during a medical emergency.

A. SYSTEM ARCHITECTURE

The mechanism and basic operating principle of the proposed ventilator is shown in the component diagram of Fig. 2. The most important key techniques are reading SpO_2 from oximeter, reading RR from impedance pneumography technique, and controlling solenoid valve. At first, the PPG signal of patient is obtained through Max30105 pulse oximeter.

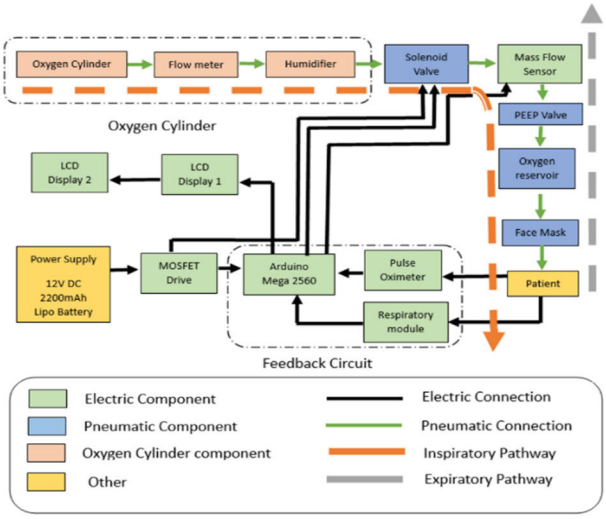

FIGURE 2. Proposed model of the ventilator.

The obtained signal is sent to the Arduino Mega microcontroller using Inter-Integrated Circuit (I2C) bus interface connection protocol. Microcontroller computes SpO_2 and heart rate from peak-to-peak interval of the PPG signal. However, RR is obtained through impedance pneumography technique using ADS1292R ECG/Respiration Module. The impedance pneumography technique records RR considering changes in bioimpedance of chest during inspiration and expiration phases. The obtained signal is sent using Serial Peripheral Interface (SPI) connection protocol to the microcontroller. These communications are made through SPI library of Arduino microcontroller board. The measured SpO_2 and RR are the inputs of the feedback system and control the ventilation modes.

The feedback mechanism is an integral part of the proposed design. The operating principle of the feedback system is shown in the flow chart of Fig. 3. A SpO_2 level above 94% is considered as a healthy level of oxygen that carries hemoglobin through the blood [31]. With a SpO_2 level above 94%, if patient experiences breathing discomfort ventilation will be provided with 1:2 I:E ratio until patient will attain conformable breathing and a SpO_2 above 97%. In other cases when the SpO_2 level is 94% and lower, the system will check RR and decide breathing parameters for ventilation. The total time cycle (TCT), inspiration time (T_i) and expiration time (T_e) can be determined from the measured RR and are defined in (1) and (2) respectively.

$$RR = \frac{60 \text{ seconds}}{TCT} \tag{1}$$

$$TCT = T_i + T_e \tag{2}$$

Standard ventilation mechanism utilizes the inspiration time (T_i) to expiration time (T_e) at a ratio of 1:2 (i.e., RR=20bpm) or 1:4 (i.e., RR=12bpm), confirming an extended time for expiration [32]. This proposed design imitates the working norms of a conventional ventilator. When SpO_2 level decreases to 94% and below, the system delivers breath based on RR value. If RR value stays above 15bpm then the selected I:E ratio is 1:2 and if RR value ranges from 12bpm to 15bpm which is less critical, and the patient will receive breaths at 1:4 I:E ratio. The inspiration time (T_i) is kept at one second because even though high T_i improves oxygenation but it causes breathing difficulties such as decrease in cardiac function, CO_2 retention, stacking of breaths, hyperinflation, barotrauma and metabolic acidosis [33]. To comprehend the working principle of this system the entire procedure can be split into three modes of operation as clarified in table 1.

TABLE 1. Ventilation mode selection based on SpO_2 and RR.

Feedback Control Parameters	Ventilation Modes		
	Mode 1 (Not Critical)	Mode 2 (Critical)	Mode 3 (Less Critical)
Oxygen Saturation (SpO_2)	>94%	≤94%	≤94%
Respiratory Rate (RR)	N/A	>15bpm	≤15bpm
Total Cycle Time (TCT)	N/A	<4sec	≥4sec
Inspiration to Expiration Ratio (I:E)	1:2	1:2	1:4

The suggested ventilator aims to function as an emergency support system, particularly in situations like the past SARS-CoV-2 pandemic. It features independent ventilation support with spontaneous breathing. To meet specific clinical performance criteria, the ventilator must undergo an evaluation

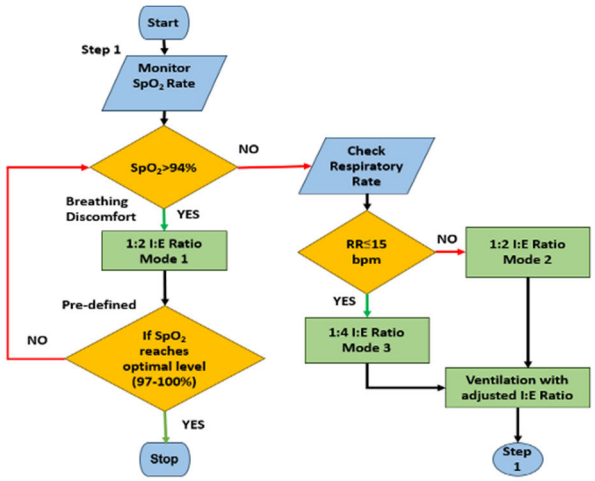

FIGURE 3. Flow chart of the proposed feedback system algorithm.

based on The Medicines and Healthcare products Regulatory Agency (MHRA) [34] guidelines. The critical operation parameters of the proposed ventilator are presented in table 2.

TABLE 2. Critical operation parameters for the developed prototype.

Parameters	MHRA	Proposed ventilator
Respiratory rate (RR)	10-30 breaths per minutes	12-20 breaths per minutes
Inspiratory to expiratory ratio (I:E)	1:1 to 1:4	1:2 and 1:4
Positive end expiratory pressure (PEEP)	5-10 cmH_2O	5 cmH_2O
Peak inspiratory flow rate (PIRF)	Up to 100 $Lmin^{-1}$	15 $Lmin^{-1}$

B. PARTICIPANTS

To evaluate how well the ventilator prototype functions under controlled conditions, it underwent testing on a bench. Twelve volunteers, aged approximately 33.9 years on average with no notable respiratory issues, participated in this assessment. Additionally, a quantitative analysis was conducted to compare the simulated respiratory rate (RR) with the actual hardware-derived RR. Furthermore, to broaden the study's scope, an additional 32 subjects, spanning ages 19 to 92, were included, irrespective of their lung health status.

C. BIO-SIGNAL RECORDING PROCEDURE

In the experimental setup volunteers were requested to place their fingertip on the Max30105 pulse oximeter for monitoring oxygen saturation. To monitor the ECG signal and the RR, electrodes were attached at fourth intercostal spaces on both right and left sternums and fifth intercostal space at the midclavicular line. Volunteers were connected to the prototype through conventional nasal mask and tubing.

D. FEEDBACK PARAMETERS MEASUREMENT

Respiratory rate (RR) and oxygen saturation (SpO_2) levels were evaluated using the ADS1292R ECG/Respiration module and Max30105, respectively. These measurements were then incorporated into the proposed device to compute the necessary I:E ratio for selecting the appropriate ventilation mode. Additionally, real-time photoplethysmography (PPG) signals were captured using MATLAB (The MathWorks Inc., Natick, MA, USA), facilitated by an Arduino interface, and processed using customized scripts. MATLAB's RR extraction algorithm was employed to determine the respiratory rate. The results of the RR extraction algorithm and SpO_2 values obtained from hardware were integrated into the Simulink ventilator model to evaluate the response within the simulation platform.

E. DATA ANALYSIS

The data gathered from the experiments were scrutinized to evaluate the functionality of the proposed ventilator. The simulation model was also evaluated using real-time data. A comparative analysis was carried out to compare the respiratory rates (RRs) obtained from both the hardware and MATLAB algorithm. Additionally, accuracy and correlation coefficients were computed to assess the performance of the ventilator.

F. ETHICAL CONSIDERATIONS

The ethical approval for the experiment has been asserted by the Ethical Review Board of American International University-Bangladesh (AIUB) which is based on declaration of Helsinki.

III. SIMULATION MODEL

This section describes the different parts of the simulation which was performed to validate the conceptual design.

A. RR EXTRACTION ALGORITHM FROM MEASURED PPG SIGNAL

Numerous studies in the literature have demonstrated the effectiveness of Discrete Fourier Transform (DWT) in extracting respiratory rate from PPG signals [35], [36], [37]. PPG signals are often non-stationary and contain various frequency components related to respiratory and cardiovascular activities. It is also susceptible to noise from multiple sources including motion artifacts and ambient light changes. DWT's ability to localize frequency information and separate signal components at different scales, allowing for the attenuation of noise at specific frequency bands makes it well-suited for extracting respiratory rate from PPG signal. DWT's ability to adapt to non-stationary signals is advantageous for respiratory rate extraction from PPG signals, as it can capture variations in respiratory patterns over time. DWT can be implemented efficiently in terms of computation, making it suitable for real-time applications, such as continuous respiratory rate monitoring. This is particularly important in healthcare settings where timely and accurate respiratory rate information is crucial. Here in this study DWT is used to extract the RR from the real time PPG signal.

DWT is used to decompose the PPG signal to obtain the frequency contents of respiratory signal. DWT is the dominant technique used for biomedical signal processing which utilizes a high pass filter (HPF) and a low pass filter (LPF) to decompose the signal into different scales. The scale (s) and translation (τ) parameters are $s = 2j$ and $\tau = k{\cdot}2j$. The DWT can be given for a signal x(t) as shown in (3) and (4).

$$W_\psi\,(s,\tau) = \int_{-\infty}^{\infty} x\,(t){\cdot}\psi_{s,\tau}\,(t)\,{\cdot}dt \tag{3}$$

$$\psi_{j,k}\,(t) = \frac{1}{\sqrt{2^j}}{\cdot}\psi\left(\frac{t - k{\cdot}2^j}{2^j}\right) \tag{4}$$

Here, $W_\psi\ (s,\tau)$, denotes the wavelet transform coefficients and $\psi_{s,\tau}(t)$ is the fundamental mother wavelet. The algorithms for determining approximation (A) and detail (D) coefficient are shown in (5) and (6).

$$A_{j,k} = \sum_n h_0 \cdot (n - 2k)\cdot A_{(j-1)k} \tag{5}$$

$$D_{j,k} = \sum_n h_1 \cdot (n - 2k)\cdot A_{(j-1)k} \tag{6}$$

The selection of wavelet is determined by the type of signal and the usage of it. An orthogonal wavelet decomposition method proved to be efficient in restoring the respiratory information intact with the PPG. Symlets [38] are compactly supported orthogonal wavelets with the least asymmetry and the highest number of vanishing moments for a given supporting width [39]. In this study, ''sym5'' wavelet was chosen as the basic function for estimating breathing information, because it has symmetric property and nice Fourier localization. Symlets also provide more accurate details and their energy spectrum is concentrated around lower frequency range.

The general RR for adults who are healthy is between 12 bpm and 20 bpm and for babies it reaches up to 60 bpm maximum [40].

So, the RR frequency range corresponds to 0.2Hz to 1Hz frequency elements of PPG signal. Level-9 decomposition is chosen as it shows low frequency components between 0.244Hz to 0.488Hz at d9 and between 0.488Hz to 0.98Hz at d8 with a sampling frequency of 125Hz.

The detailed block diagram of the R peak detection process is shown in Fig. 4. All other coefficients except d8 and d9 are ignored to obtain the expected result. After performing DWT detail coefficients are selected and with inverse DWT the respiratory signal is generated. A threshold is considered from the magnitude of the inverse DWD signal to identify the R peaks in simulated respiration signal.

From that respiratory signal, the number of amplitude (R peaks) is determined in 10 seconds. The respiratory rate (RR) is defined by (7).

$$RR = \frac{60\text{ seconds}}{10\text{ seconds}}{\cdot}\text{Peaks in 10 seconds} \tag{7}$$

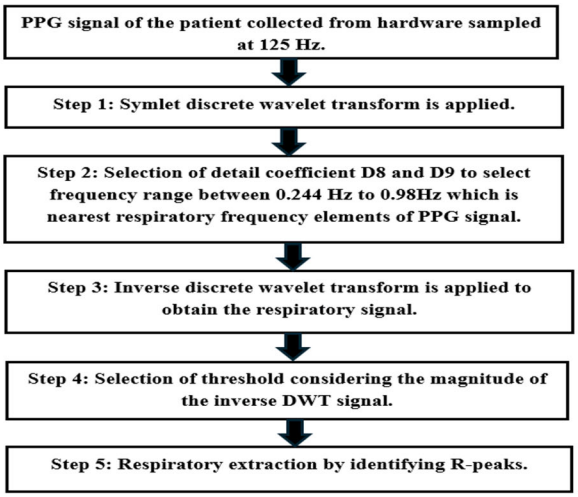

FIGURE 4. RR extraction technique using discrete wavelet transform.

B. SIMULINK MODEL OF THE VENTILATOR

The Simulink model of the proposed ventilator is shown in Fig. 5 This model works as a reference to validate the hardware. Here in the simulation model the pressure signal is the control signal that provides the required I:E ratio for this ventilator. Based on a real-life breathing pattern of a healthy adult, the pressure signal is generated using MATLAB functions which is shown in Fig. 6. The pressure signal and ventilation parameters are kept same for both I:E ratios except the expiratory time T_e.

The setting pressure and PEEP are set at 25cmH_2O and 5cmH_2O respectively. The rising time α, is the time to develop the peak airway pressure (P_{aw}) or the plateau pressure and is proportional to flow.

A smaller rise time can ensure high flow at the beginning of the inspiration. The device here is designed for non-critical patients so force ventilation is not required and hence the plateau pressure was maintained at 30 cm H_2O considering the maximum distending pressures of lung which is 25 - 35 cm H_2O [23]. Setting pressure is taken considering the PEEP up to 25 cm H_2O to reach the preferred tidal volume of 500mL. An equivalent electric model of a multi compartmental lung was considered in this study, which was proposed in literature by Koo [12] and Al-Naggar [41]. The circuit was simulated to generate continuous time varying waveforms of volume (V), flow (F) and pressure (P). For 20bpm RR, complete 8 respiratory cycles were demonstrated in Fig. 7.

The peak inspiratory flow rate (PIFR) is maintained at 100L/min to generate a breath with a tidal volume of 500mL. In modern ventilators a range between 60 L/min to 120 L/min PIFR is kept for maintaining tidal volume from 400mL to 500mL which is the requirement of a healthy adult [42]. Due to the properties of lung, peak expiratory flow rate (PEFR) is kept higher compared to PIFR. During the inspiratory time which is 1 second the tidal volume reaches to 500mL and

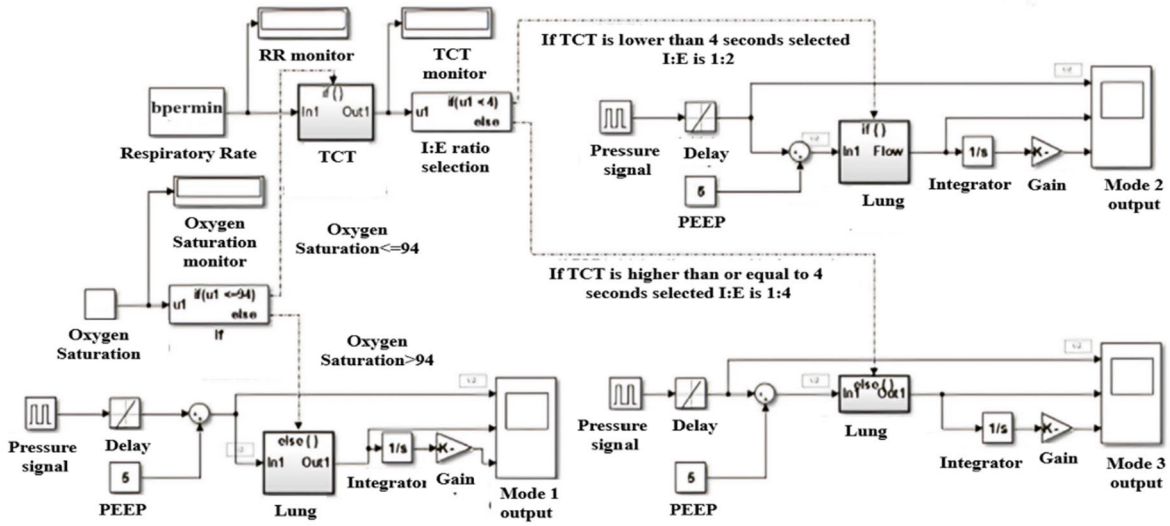

FIGURE 5. SIMULINK model of the designed ventilator [30].

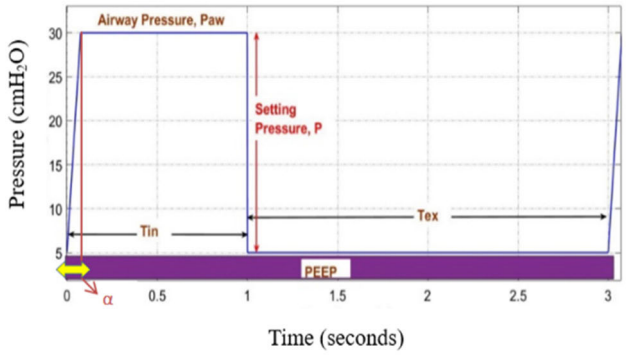

FIGURE 6. Simulated pressure signal considering I:E ratio at 1:2 [30].

during the 2 seconds of expiratory time PEEP volume which is near about 100mL will be available in the airway. The hardware model mirrors the proposed simulation model depicted in Fig. 8. The SpO2 level is derived from the Max30105 pulse oximeter. The control of the inspiration-to-expiration (I:E) phase is managed by a solenoid valve, which responds to feedback from SpO2 and RR data sent to the microcontroller. Connecting to the microcontroller, the solenoid valve is facilitated through a MOSFET power driver, operating at 12V. Additionally, the microcontroller and sensors require 5V to function.

IV. HARDWARE IMPLEMENTATION

A 12V to 5V step down power module is used to power up all these components. All the data extracted from the patient and ventilator's current state are projected on two LCD displays connected to the microcontroller utilizing I2C shared bus. The 4 × 16 LCD shows HR, SpO_2, and RR, while 2 × 16 LCD shows the I:E ratio. The implemented ventilator box has one inlet and one outlet. The inlet is connected to the oxygen cylinder section. The oxygen cylinder is refilled at a pressure of 2200 psi and is equipped with a valve knob connection to a pressure gauge meter. The oxygen flows through a flow meter where the flow rate can be controlled in L/min unit. Subsequently, the oxygen is directed into a humidifier bottle where it is mixed with water, thereby enhancing its moisture content. The flow pipe serves as a conduit for delivering oxygen with increased humidity.

Finally, the pipe is connected to the inlet of the ventilator box, facilitating the proper functioning of the implemented system. The outlet of the ventilator box is connected to a breathing circuit comprising an O_2 reservoir, a PEEP valve for controlling end-expiratory pressure, and a breathing tube. The regulated oxygen is efficiently conveyed through the breathing tube to the patient's face mask, ensuring optimal delivery and administration by the microcontroller using the feedback system.

V. RESULT AND DISCUSSION

In this section data analysis is shown according to the sequence given in methodology subsection E.

A. HARDWARE PERFORMANCE ASSESSMENT

The prototype was evaluated in a bench test, which was carried out on 12 volunteers with mean age 33.9±10.9 years and none of them reported any significant respiratory illness.

In the experimental setup volunteers were requested to place their fingertip on the pulse oximeter for monitoring oxygen saturation. To monitor the ECG signal and the RR electrodes were attached. Volunteers were connected to the prototype through conventional nasal mask and tubing, with adjusted inspiratory and expiratory flow rate as shown in Fig.9.

The flow of the oxygen was controlled by mass flow sensor which was kept constant during experiment considering any

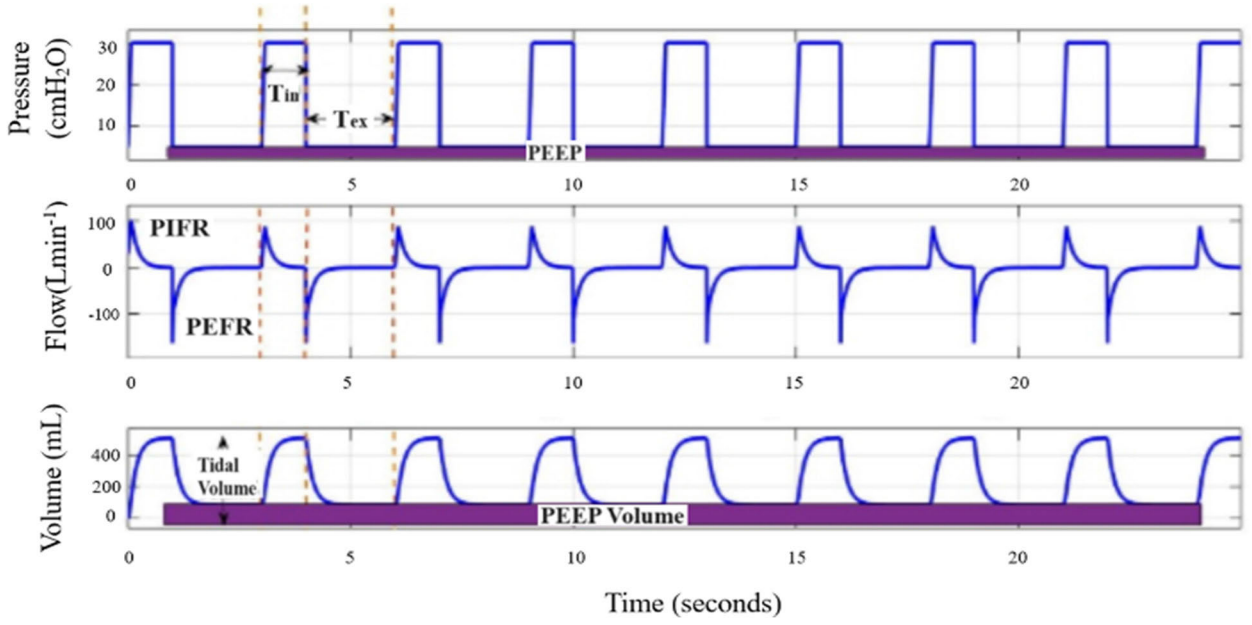

FIGURE 7. Outputs from simulation of lung model; pressure in cm H_2O, flow in L/min, and volume in ml waveforms with 5 cm H_2O PEEP [30].

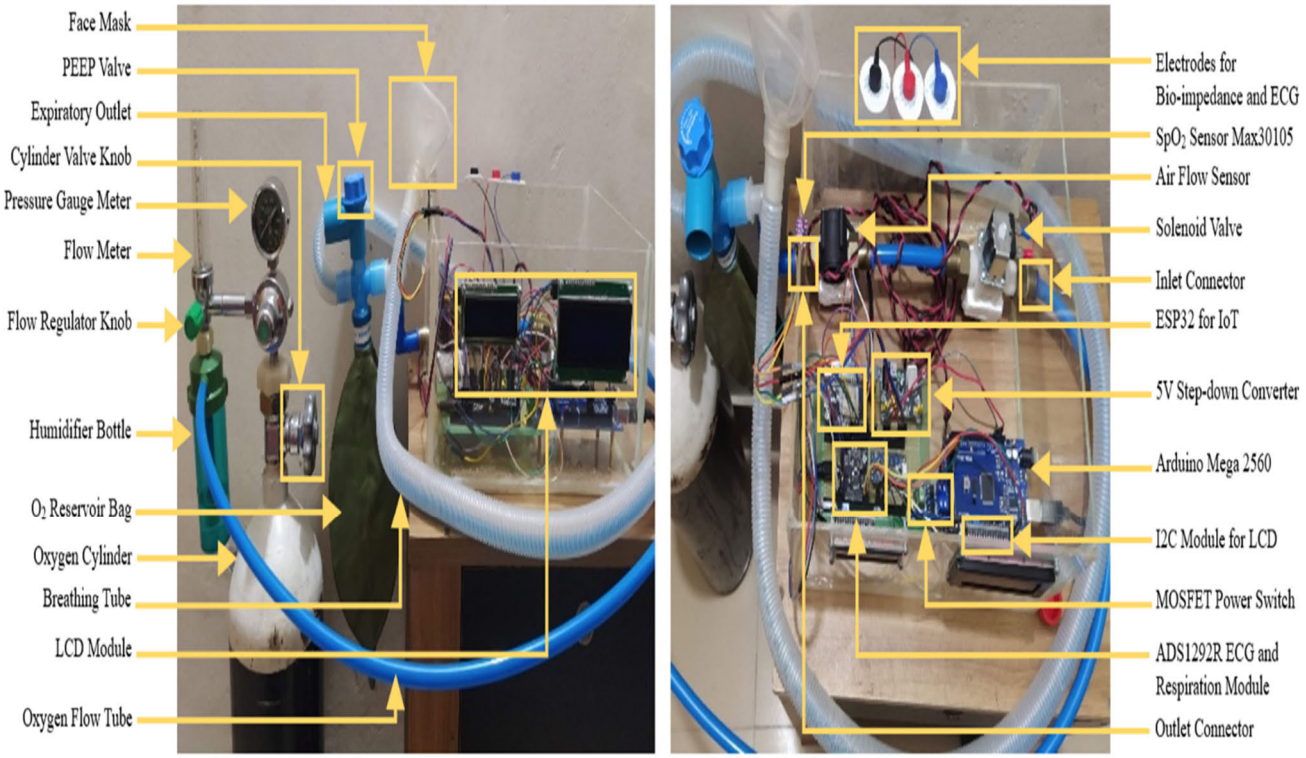

FIGURE 8. Ventilator hardware implementation. (a) Front view and (b) Top view.

unintended leak due to technical specifications. The peak flow rate of the prototype was titrated at 15 L/min. The PEEP valve always maintained at 5 cmH_2O continuous pressure in the airway. During the experiment, volunteers were requested to increase their airway resistance and to decrease their respiratory compliance by mimicking a purely obstructive patient and a purely restrictive patient respectively. Subsequently, each subject was instructed to breathe for 2 min by simulating

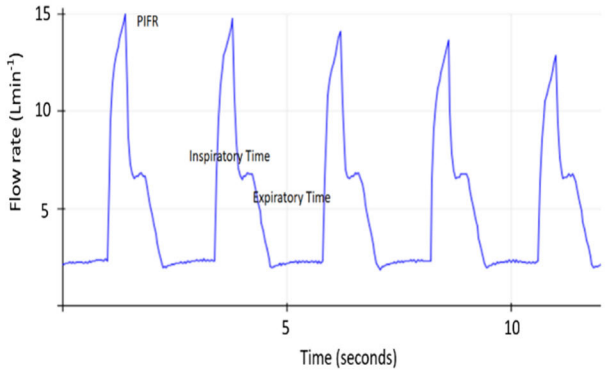

FIGURE 9. Sample tracing of flow rate during ventilation collected from Arduino IDE plotter.

TABLE 3. Respiratory parameters derived by the systems of 9 different lung conditions simulated for the bench test and ventilator mode selection.

Lung Condition	Simulated Patient	SpO_2 level	RR breaths/min	I:E	Ventilator mode
Mild	1	96%	12	1:2	Mode 1
	2	99%	12	1:2	Mode 1
	3	98%	16	1:2	Mode 1
Obstructive	1	91%	24	1:2	Mode 2
	2	93%	18	1:2	Mode 2
	3	89%	30	1:2	Mode 2
Restrictive	1	95%	12	1:2	Mode 1
	2	88%	20	1:2	Mode 2
	3	90%	14	1:4	Mode 3

different lung loading conditions. The outcome is shown in table 3.

For mild patient group it is noticed that when the SpO_2 level of the patient is above 94% the system delivers mode 1 ventilation, and it does not response to the RR value even if it is higher than 15bpm. In case of obstructive patient group, due to having lower SpO_2 than 94% and higher RR above 15bpm, mode 2 ventilation was selected. The restrictive group received both mode 3 and mode 2 ventilation based on their SpO_2 and RR.

In Fig. 10(a), PPG Signal measured by hardware is shown with oxygen saturation level. This signal was obtained through pulse oximeter sensor MAX30105 sensor. The Integrated development environment (IDE) is used here for both analyzing and visualizing data. PPG technique utilizes the absorption difference and computes the oxygen saturation level in percentage. Respiration rate was measured by ADS1292R ECG/Respiration module which uses impedance pneumography technique that measures the change in bioimpedance of chest during inspiration and expiration phases. The heart rate, RR, ECG signal and respiratory signal are the outputs of the module which is shown in Fig. 10(b).

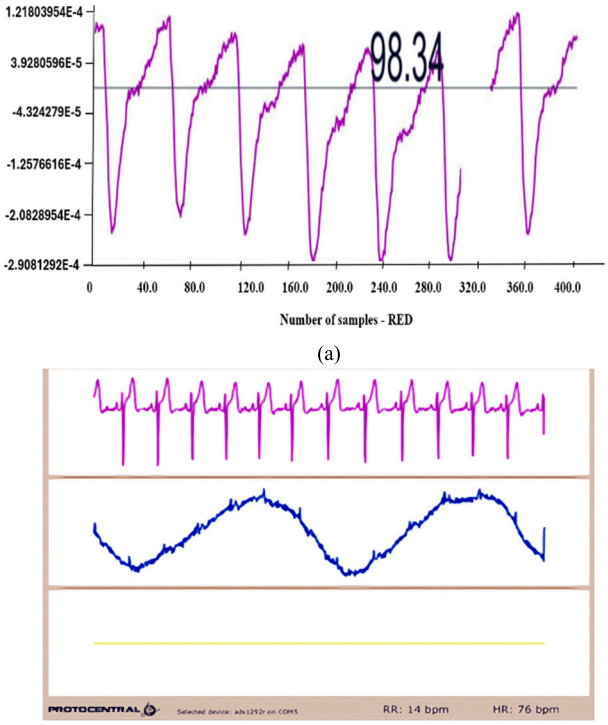

FIGURE 10. Feedback parameter measurement by hardware. (a) PPG signal with SpO_2 level 98.34% and (b) ECG signal and respiratory signal with RR & heart rate.

Two LCD displays were integrated to display all the extracted biofeedback data such as heart rate, SpO_2 level, RR, and I:E ratios as show in Fig.11. Here all the ventilation modes of table1 are shown in hardware.

B. SIMULATION MODEL OUTCOME

The real time PPG and respiratory signals of the subject groups were also collected during the bench test to evaluate the simulation model performance. Initially raw PPG signals were imported into the data acquisition tool MATLAB with the help of Arduino interface and were processed with custom scripts.

After being processed with moving average filters to reduce baseline wander, muscle artifacts, and other high-frequency noise components, the PPG signal was sampled at 125 Hz. The processed PPG signal was fed to the feedback algorithm to extract the RR of the subject. PPG derived RR and real time SpO_2 were given to the simulation model as inputs to compare the outcomes with the prototype. The outcome of the simulation model for ventilation mode 1 is shown in Fig. 12. When SpO_2 goes below 94%, system starts the RR estimation. If the RR value is higher than 15 bpm, the ventilation mode 2 is initiated which is shown in Fig. 13. In ventilation mode 2 the 1:2 I: E ratio was selected, and breaths at a greater number are supplied within 60 seconds to the patient.

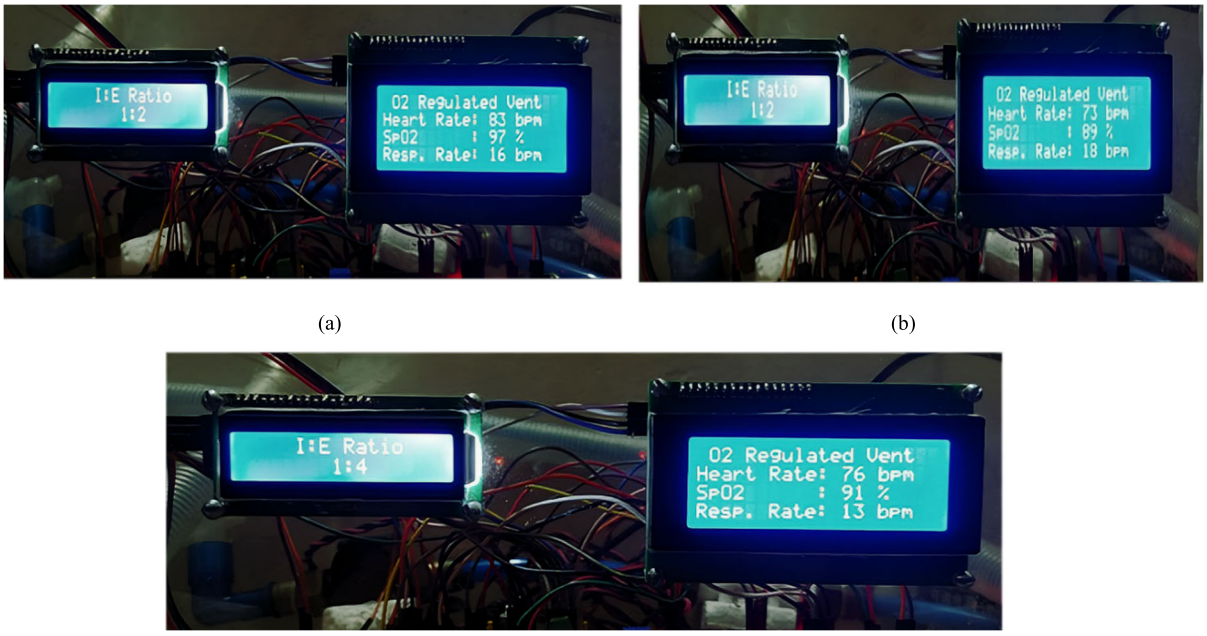

FIGURE 11. Hardware outcomes to supply different modes of ventilation according to table 1. (a) Mode 1; The SpO_2 > 94% so selected I:E ratio is 1:2 (b) Mode 2; The SpO_2 ≤ 94% and RR > 15bpm so selected I:E ratio is 1:2 and (c) Mode 3; The SpO_2 ≤ 94% and RR≤15bpm so selected I:E ratio is 1:4.

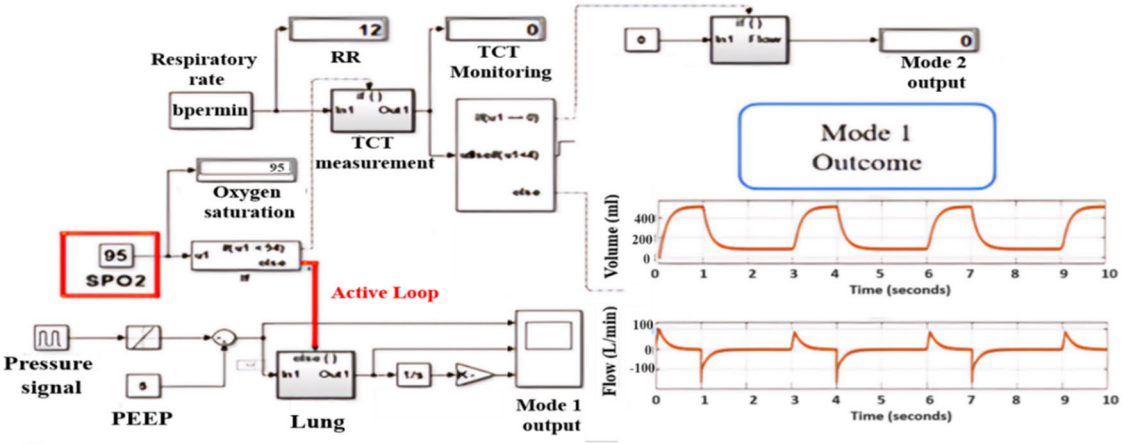

FIGURE 12. Simulink model for ventilation mode 1 when SpO_2 is higher than 94% and RR is less than 15bpm.

When the SpO_2 level is lower than 94% but RR is less than 15bpm, the ventilator selects breathing rate at 1:4 I:E ratio. The simulink model for mode 3 ventilation is shown in Fig.14 where SpO_2 is below 94%, RR is less than 15bpm. The Fig.15 demonstrates that the simulated and hardware derived respiratory signals exhibit an equal number of peaks, their respective respiratory rates (RRs) are also identical. The acquired respiration signal from hardware is considered as reference signal. The PPG derived respiratory rate is visually equivalent to the measured respiration signal.

C. COMPARISON OF CALCULATED RR FROM THE HARDWARE AND SIMULATION

A quantitative analysis has also been done to compare between PPG signal derive RR and measured RR where 40 subjects were selected within the age range between 19 years to 92 years. The individuals were categorized under two different age groups, irrespective of their gender and respiratory condition. Group 1 consisted of 20 adults with ages below and equal to 50 years and group 2 with age above 50 years. In table 4 comparison between the PPG signal derived RR (RR_derived) and measured RR (RR_reference) is shown in terms of mean ± standard deviation (SD) using (9) and (10).

$$\text{Absolute error} = |\text{Reference}_{RR} - \text{Derived}_{RR}| \tag{8}$$

$$\textbf{MAPE} = \frac{1}{n}\sum_{i}\frac{|\text{Reference}_{RR} - \text{Derived}_{RR}|}{\text{Reference}_{RR}} \cdot 100\% \tag{9}$$

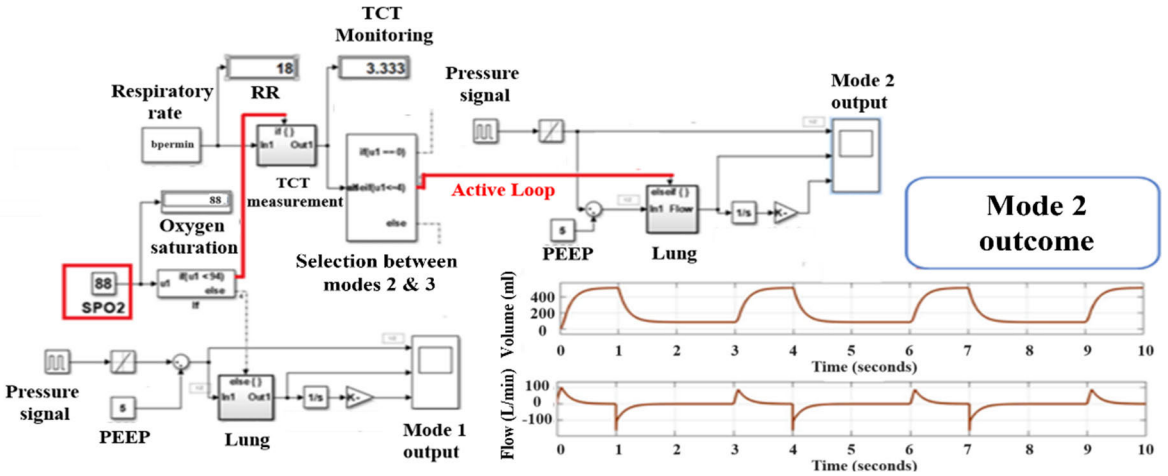

FIGURE 13. Simulink model for ventilation mode 2 when SpO_2 is below 94%, RR is above 15bpm.

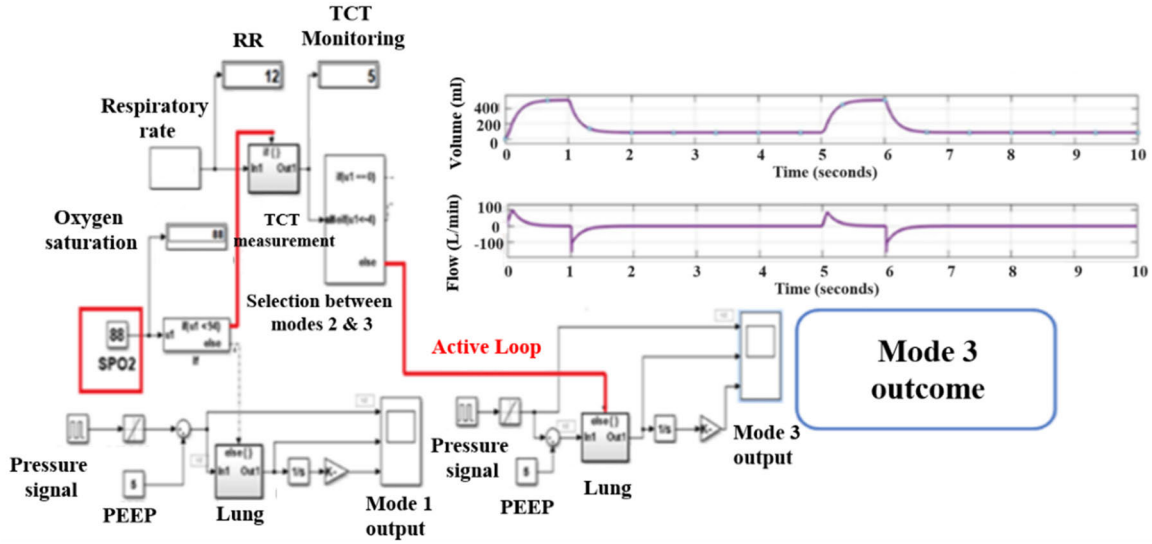

FIGURE 14. Simulink model for ventilation mode 3 when SpO_2 is below 94%, RR is less than 15bpm.

TABLE 4. Comparison between reference and derived RR.

Age Group	RR Data Type	RR (Mean±SD) in bpm	Absolute Error (Mean±SD) in bpm	MAPE (%)
Grp_1	RR_reference	17.5±0.042	0.558±0.64	8.64
	RR_derived	18±0.0465		
Grp_ 2	RR_reference	19.2±0.062	0.417±0.59	7.91
	RR_derived	20.6±0.062		

The maximum absolute errors for group 1 and group 2 are 1.2 bpm and 1.007 bpm respectively. For both groups the mean absolute percentage errors (MAPE) were found below 10% shown in table 4.

Box-whiskers plots of RR_derived and RR_reference for two age groups is demonstrated in Fig. 16. Here it is found that the RR_reference was coincidental with RR_derived. Box-Whisker plot of age group up-to 50 years shows that the median (median (RR_Reference) = 18, median (RR_Derived) = 18) and inter quartile range (IQR) (IQR(RR_Reference) = 6, IQR(RR_Derived) = 6) are exactly same for both reference and derived RR whereas for age group above 50 are nearly equal. For the age group above 50 years the deviation in median and IQR is more than 10%. These results indicated that the Derived RR is more comparable to the Reference RR for younger age group.

The Bland–Altman plots are given in Fig.17 to assess the agreement amongst the reference and derived RR. For both the groups reference and derived RR showed good agreement. For age group up to 50 years the difference values are firmly

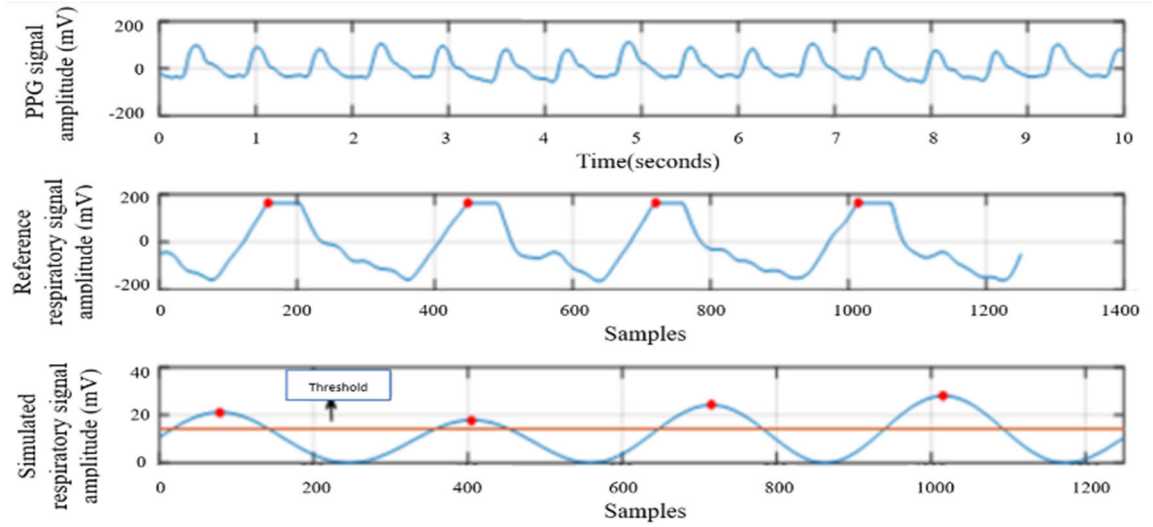

FIGURE 15. Outcome of the sym5 DWT method and designed hardware to compare the values of respiratory rate (RR).

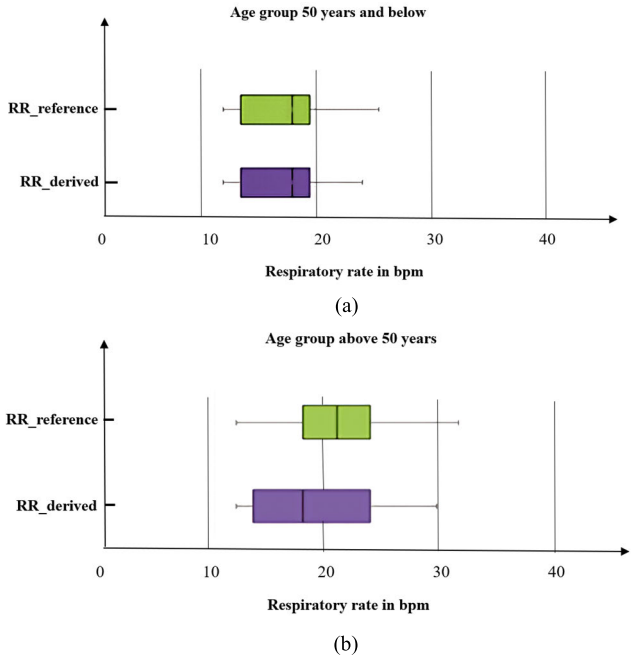

FIGURE 16. Box-Whisker's plot; (a) Age group up to 50 years and (b) Age group above 50 years.

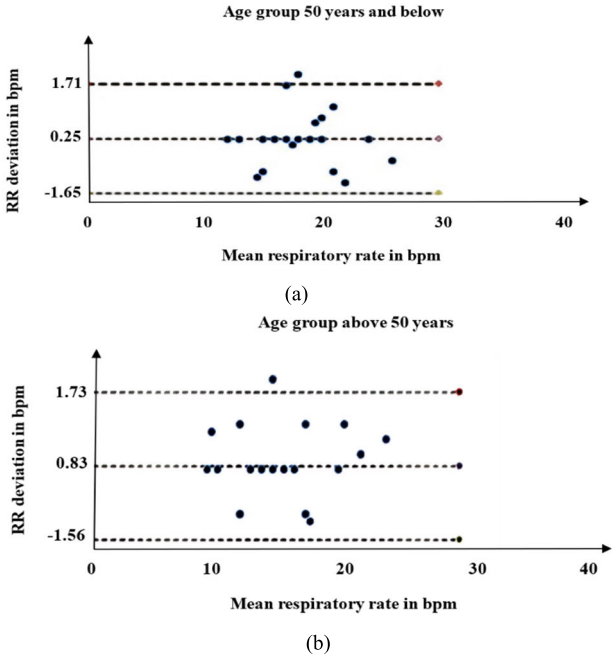

FIGURE 17. Bland-Altman plot for subject groups; (a) Age group up to 50 years and (b) Age group above 50 years.

arranged around the minor bias 0.025 within 95% limit of agreement (−1.66, 1.71), which contains 95% of the difference scores (19/20).

For age group above 50 years though the bias (0.83) value is slightly larger than former group, but the limit of agreement (−1.56, 1.73) contains similar difference scores. It means that the difference values are firmly arranged around the mean bias within the limit of agreement (i.e., mean ±1.96 ×SD) for both groups.

Therefore, derived RR can be used interchangeably with the reference RR and provide reliable results for both age groups. From these plots, it is also observed that the spread in deviation is almost similar for both age groups.

D. MODE SELECTION EVALUATION

One of the crucial challenges for the ventilator is to select the I:E ratio when SpO_2 level decreases below 94%. This condition occurs for more critical patients when ventilator selects mode between mode 2 and mode 3 as shown in table 1. By selecting these modes, the system supplies breaths according to the requirement of the patients for ensuring lung

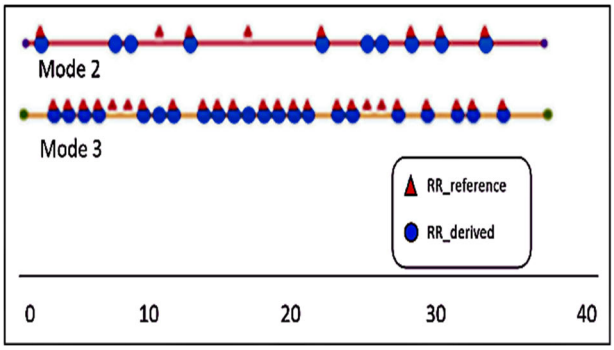

FIGURE 18. Outcome of the case selection experiment.

protective ventilation. So, it is necessary to select modes precisely for this group of patients. Therefore, the accuracy of mode selection has been observed for the system. Both derived and reference RR were recorded for 32 subjects with SpO_2 level below 94% and the outcome is shown in Fig.18. It is seen from the plot that out of 32 individuals, disagreement occurs between hardware and simulation model for 6 patients only to identify appropriate mode between mode 2 and mode 3 which ensures the mean accuracy of 81.25% according to (10).

$$\text{Accuracy} = \frac{\text{Numer of correct prediction}}{\text{Total number of prediction}} \cdot 100\% \qquad (10)$$

The correlation coefficient (CC) is 0.78 which shows a moderately correct decision-making capability of the ventilator based on its feedback mechanism.

E. COMPARISON WITH THE EXISTING LITERATURE

In the following analysis, a comprehensive comparison of various ventilator models is presented in the form of a table. Table 5 has been curated to highlight key features, specifications, and design characteristics of each model which serves as a useful reference point for evaluating and contrasting the proposed ventilator design. While all four ventilator designs of table 5, including proposed model, showcase commendable innovations, Proposed ventilator stands out for several reasons. The inclusion of a single solenoid valve in the CPAP model, coupled with a versatile Arduino Mega 2560 microcontroller ensures efficient and precise control over the ventilation process.

The incorporation of vital monitoring, such as ECG, PPG, HR, RR, and SpO_2, showcases a comprehensive approach to patient care. The integration of a feedback mechanism for I:E ratio adjustment based on illness severity demonstrates a sophisticated adaptive capability, enhancing the ventilator's responsiveness to varying patient conditions.

Furthermore, the utilization of a 12V DC, 2200mAH Lipo battery provides a practical and portable power solution. The proposed ventilator excels in its ability to combine advanced technology with practical features, making it a standout choice in non-invasive ventilation solutions.

TABLE 5. Comparison among the available portable non-invasive ventilators available in literature.

Features	Bhoyar et al. (2021) [9]	Madekurozwa et al. (2021) [5]	Arshad et al. (2023) [18]	Proposed Model
Ventilator type	BVM based	CPAP (4 solenoid valve-based)	High-pressure turbine-based (CPAP and BiPAP)	CPAP (1 solenoid valve-based)
Power supply requirement	12V DC, 30A, 360W	24V DC, 70W	24V DC, 43.2W	12V DC, 2200mAH
Micro controller	No required	TEENSY microcontroller board	Raspberry pi pico micro-controller	Arduino Mega 2560 micro-Controller
Sensors	Not required	Pressure sensor Omegadyne (PXM319) Oxygen sensor Teledyne (R-22MED)	Gauge Pressure sensor (Honeywell HSC) Mass flow meters (SFM3300, Sensirion AG)	SpO_2 (MAX30105) Mass Flow sensor (Winsen F1031v) RR (ADS1292R)
Valves used	Non-rebreathing valve	4 solenoid valves	Non return valve Membrane valve	1 solenoid valve 1 PEEP valve
Ventilation mode	Not available	CPAP	CPAP, BiPAP	CPAP
I:E ratio adjustment range	Not available	1:2 and 1:4	1:1 to 1:4	1:2 and 1:4
Additional body vitals monitoring	Not available	Not available	Not available	ECG, PPG, HR, RR , SpO_2
Feedback control	Not available	Not available	Not available	Yes

F. LIMITATION OF THE WORK AND FUTURE SCOPES

The prototype in its present state is not devised to check all ventilator parameters and also delivers oxygen supply at a constant flow rate for all group of patients. Moreover, the proposed feedback mechanism can only control the I:E ratio between 1:2 and 1:4. In the course of the study, it has become evident that the current set of instruments, while providing valuable insights but further enhancements in instrumentation are necessary to refine the accuracy and efficiency by monitoring and controlling more ventilatory parameters such as tidal volume, PIFR, PEFR, plateau pressure, respiratory resistance-compliance, fraction of inspired oxygen (FiO_2) and etc. A refine and acute feedback mechanism may be achieved by a holistic framework for the analysis of such parameter-dependent multi-modal complex systems. Hence introducing statistical machine learning models [43], [44] can be incorporated for enhancing control on both ventilation mode and ventilatory parameters. Furthermore, incorporating IoT technology can enhance the device's performance by enabling remote monitoring and management of non-invasive ventilation therapy. The ongoing efforts to improve and upgrade the instrumentation, a thorough cost assessment will be included in future iterations of this research.

VI. CONCLUSION

Developing a non-invasive ventilator that operates effectively in critical situations poses a significant challenge. The focus of this study is on creating a system that extracts vital control parameters—SpO2 and RR—from the patient's biosignals to regulate ventilation. This non-invasive ventilation (NIV) system demonstrates substantial synchrony, prioritizing patient-centric ventilation to enhance comfort and mimic natural breathing patterns. By extending expiration

time from 2 to 4 seconds, the system allows for more thorough exhalation, further improving patient experience.

Extensive testing across various respiratory conditions, in both real-time and simulated environments, validates the system's performance. Ethical approval and validation from local review boards, alongside data gathered from human participants, underpin its reliability. This system emerges as a promising alternative to oxygen therapy for patients experiencing mild respiratory distress due to ARDS and COPD. Its minimal requirement for medical personnel intervention makes it suitable for home and long-term care settings.

Additionally, the system holds potential for managing sleep-related respiratory conditions, expanding its utility. With a focus on affordability, the proposed ventilator aims to minimize costs, enabling widespread accessibility even in resource-constrained regions. Future iterations could incorporate additional features for enhancement, while adherence to regulatory standards ensures safety and efficacy. Using affordable and accessible components, the projected cost remains competitive compared to current ventilators, fostering prospects for mass production and global distribution which helps to improve respiratory support in underserved communities worldwide.

REFERENCES

[1] G. Bellani et al., "Noninvasive ventilatory support of patients with COVID-19 outside the intensive care units (WARd-COVID)," *Ann. Amer. Thoracic Soc.*, vol. 18, no. 6, pp. 1020–1026, Jun. 2021, doi: 10.1513/annalsats.202008-1080oc.

[2] F. Menzella, C. Barbieri, M. Fontana, C. Scelfo, C. Castagnetti, G. Ghidoni, P. Ruggiero, F. Livrieri, R. Piro, L. Ghidorsi, G. Montanari, G. Gibellini, E. Casalini, F. Falco, C. Catellani, and N. Facciolongo, "Effectiveness of noninvasive ventilation in COVID-19 related-acute respiratory distress syndrome," *Clin. Respiratory J.*, vol. 15, no. 7, pp. 779–787, Mar. 2021, doi: 10.1111/crj.13361.

[3] A. Mukhtar, A. Lotfy, A. Hasanin, I. El-Hefnawy, and A. El Adawy, "Outcome of non-invasive ventilation in COVID-19 critically ill patients: A retrospective observational study," *Anaesthesia Crit. Care Pain Med.*, vol. 39, no. 5, pp. 579–580, Oct. 2020, doi: 10.1016/j.accpm.2020.07.012.

[4] R. M. Kacmarek, "Current status of new modes of mechanical ventilation," *Can. Respiratory J.*, vol. 3, no. 6, pp. 357–360, 1996, doi: 10.1155/1996/248358.

[5] M. Madekurozwa et al., "A novel ventilator design for COVID-19 and resource-limited settings," *Frontiers Med. Technol.*, vol. 3, Oct. 2021, Art. no. 707826, doi: 10.3389/fmedt.2021.707826.

[6] M. M. Khan and S. R. Parab, "Concept and prelimnary design of an economical bag valve mask compressor as a prototype for simple ventilator during COVID-19," *Indian J. Otolaryngol. Head Neck Surg.*, vol. 74, no. S2, pp. 2878–2882, Oct. 2022, doi: 10.1007/s12070-021-02445-8.

[7] E. Castro-Camus, J. Ornik, C. Mach, G. Hernandez-Cardoso, B. Savalia, J. Taiber, A. Ruiz-Marquez, K. Kesper, S. Konde, C. Sommer, J. Wiener, D. Geisel, F. Hüppe, G. Kräling, P. Mross, J. Nguyen, T. Wiesmann, B. Beutel, and M. Koch, "Simple ventilators for emergency use based on bag-valve pressing systems: Lessons learned and future steps," *Appl. Sci.*, vol. 10, no. 20, p. 7229, Oct. 2020, doi: 10.3390/app10207229.

[8] E. Calilung, J. Española, E. Dadios, A. Culaba, E. Sybingco, A. Bandala, R. R. Vicerra, A. B. Madrazo, L. G. Lim, R. K. Billones, S. Lopez, D. D. Ligutan, J. Palingcod, and C. J. P. Castillo, "Design and development of an automated compression mechanism for a bag-valve-mask-based emergency ventilator," in *Proc. IEEE 12th Int. Conf. Humanoid, Nanotechnol., Inf. Technol., Commun. Control, Environ., Manage. (HNICEM)*, Dec. 2020, pp. 1–6, doi: 10.1109/HNICEM51456.2020.9400150.

[9] A. D. Bhoyar, "Design construction and performance test of a low-cost pandemic ventilator for breathing support," *Int. J. Res. Appl. Sci. Eng. Technol.*, vol. 9, no. 8, pp. 2374–2380, Aug. 2021, doi: 10.22214/ijraset.2021.37771.

[10] A. M. Al Husseini, H. J. Lee, J. Negrete, S. Powelson, A. T. Servi, A. H. Slocum, and J. Saukkonen, "Design and prototyping of a low-cost portable mechanical ventilator," *J. Med. Devices*, vol. 4, no. 2, Jun. 2010, Art. no. 027514, doi: 10.1115/1.3442790.

[11] O. Garmendia, M. A. Rodríguez-Lazaro, J. Otero, P. Phan, A. Stoyanova, A. T. Dinh-Xuan, D. Gozal, D. Navajas, J. M. Montserrat, and R. Farré, "Low-cost, easy-to-build noninvasive pressure support ventilator for under-resourced regions: Open source hardware description, performance and feasibility testing," *Eur. Respiratory J.*, vol. 55, no. 6, Jun. 2020, Art. no. 2000846, doi: 10.1183/13993003.00846-2020.

[12] M. C. Khoo, *Physiological Control Systems: Analysis, Simulation, and Estimation*. Hoboken, NJ, USA: Wiley, 2018.

[13] R. L. Read. (Apr. 1, 2020). *The Open Source Ventilator Game Has Changed: AmboVent and Medtronic COVID-19 Ventilators Open Sourced*. Accessed: Dec. 16, 2023. [Online]. Available: https://robertleeread.medium.com/the-open-source-ventilator-game-has-changed-ambovent-and-medtronic-covid-19-ventilators-open-d645bde594cc

[14] M. Shahid, "Prototyping of artificial respiration machine using AMBU bag compression," in *Proc. Int. Conf. Electron., Inf., Commun. (ICEIC)*, Jan. 2019, pp. 1–6, doi: 10.23919/ELINFOCOM.2019.8706360.

[15] M. Fogarty, J. Orr, D. Westenskow, L. Brewer, and D. Sakata, "Electric blower based portable emergency ventilator," in *Proc. Utah Space Grant Consortium*, May 2013, pp. 1–5. [Online]. Available: https://digitalcommons.usu.edu/spacegrant/2013/Session4/2

[16] H. Jürß, M. Degner, and H. Ewald, "A new compact and low-cost respirator concept for one way usage," *IFAC-PapersOnLine*, vol. 51, no. 27, pp. 367–372, Jan. 2018, doi: 10.1016/j.ifacol.2018.11.612.

[17] T. P. Anh, H. V. Duy, H. D. Viet, D. T. Khanh, T. L. H. Phuong, and C. D. Thanh, "Research and development of a ventilator with air pump technology," *J. Mech. Eng. Res. Develop.*, vol. 44, no. 9, pp. 134–139, 2021. Accessed: Dec. 16, 2023. [Online]. Available: https://jmerd.net/09-2021-134-139/.pdf

[18] M. Arshad, K. Mehmood, and I. Lazoglu, "Development of a non-invasive ventilator for emergency and beyond," *Comput. Biol. Med.*, vol. 167, Dec. 2023, Art. no. 107670, doi: 10.1016/j.compbiomed.2023.107670.

[19] J. Morris, J. Schofield, C. Bull, A. Knott, F. Farrow-Dunn, P. Proctor, and P. Shore, "Dynamic collaboration in a crisis: Creating a low-cost ventilator and test facility," *Meas. Sci. Technol.*, vol. 34, no. 3, Dec. 2022, Art. no. 034003, doi: 10.1088/1361-6501/aca495.

[20] H. Wang, Q.-Y. Zhao, J.-C. Luo, K. Liu, S.-J. Yu, J.-F. Ma, M.-H. Luo, G.-W. Hao, Y. Su, Y.-J. Zhang, G.-W. Tu, and Z. Luo, "Early prediction of noninvasive ventilation failure after extubation: Development and validation of a machine-learning model," *BMC Pulmonary Med.*, vol. 22, no. 1, p. 304, Aug. 2022, doi: 10.1186/s12890-022-02096-7.

[21] A. Kumar, K. Abhishek, C. Chakraborty, and N. Kryvinska, "Deep learning and Internet of Things based lung ailment recognition through coughing spectrograms," *IEEE Access*, vol. 9, pp. 95938–95948, 2021, doi: 10.1109/ACCESS.2021.3094132.

[22] M. B. P. Amato, M. O. Meade, A. S. Slutsky, L. Brochard, E. L. V. Costa, D. A. Schoenfeld, T. E. Stewart, M. Briel, D. Talmor, A. Mercat, J.-C.-M. Richard, C. R. R. Carvalho, and R. G. Brower, "Driving pressure and survival in the acute respiratory distress syndrome," *New England J. Med.*, vol. 372, no. 8, pp. 747–755, Feb. 2015, doi: 10.1056/nejmsa1410639.

[23] R. G. Brower, M. A. Matthay, A. Morris, D. Schoenfeld, B. T. Thompson, and A. Wheeler, "Ventilation with lower tidal volumes as compared with traditional tidal volumes for acute lung injury and the acute respiratory distress syndrome," *New England J. Med.*, vol. 342, no. 18, pp. 1301–1308, 2000, doi: 10.1056/NEJM200005043421801.

[24] E. Fan et al., "An official American Thoracic Society/European Society of Intensive Care Medicine/Society of Critical Care Medicine clinical practice guideline: Mechanical ventilation in adult patients with acute respiratory distress syndrome," *Amer. J. Respiratory Crit. Care Med.*, vol. 195, no. 9, pp. 1253–1263, May 2017, doi: 10.1164/rccm.201703-0548st.

[25] A. Carlucci, L. Pisani, P. Ceriana, A. Malovini, and S. Nava, "Patient-ventilator asynchronies: May the respiratory mechanics play a role?" *Crit. Care*, vol. 17, no. 2, p. R54, 2013, doi: 10.1186/cc12580.

[26] B. Ergan, J. Nasiłowski, and J. C. Winck, "How should we monitor patients with acute respiratory failure treated with noninvasive ventilation?" *Eur. Respiratory Rev.*, vol. 27, no. 148, Apr. 2018, Art. no. 170101, doi: 10.1183/16000617.0101-2017.
[27] G. Cammarota, R. Simonte, and E. De Robertis, "Comfort during non-invasive ventilation," *Frontiers Med.*, vol. 9, Mar. 2022, Art. no. 874250, doi: 10.3389/fmed.2022.874250.
[28] E. F. Hansen, C. S. Bech, J. Vestbo, O. Andersen, and L. M. Kofod, "Automatic oxygen titration with O2matic® to patients admitted with COVID-19 and hypoxemic respiratory failure," *Eur. Clin. Respiratory J.*, vol. 7, no. 1, Jan. 2020, Art. no. 1833695, doi: 10.1080/20018525.2020.1833695.
[29] (Oct. 11, 2022). *Summary | O2matic PRO 100 for Optimising Oxygen Treatment in Respiratory Conditions | Advice | NICE*. Accessed: Sep. 19, 2023. [Online]. Available: https://www.nice.org.uk/advice/mib308/chapter/summary
[30] R. Faiz, N. N. Alam, and M. H. Imam, "Design of an automated non-invasive electromechanical ventilator with feedback mechanism," in *Proc. IEEE 3rd Global Conf. Life Sci. Technol. (LifeTech)*, Mar. 2021, pp. 324–328.
[31] L. Baboi, F. Subtil, and C. Guérin, "A bench evaluation of fraction of oxygen in air delivery and tidal volume accuracy in home care ventilators available for hospital use," *J. Thoracic Disease*, vol. 8, no. 12, pp. 3639–3647, Dec. 2016, doi: 10.21037/jtd.2016.12.64.
[32] R. P. Mlcak, S. D. Hegde, and D. N. Herndon, "Respiratory care," in *Total Burn Care*, 4th ed., D. N. Herndon, Ed. London, U.K.: W. B. Saunders, 2012, pp. 239–248, doi: 10.1016/B978-1-4377-2786-9.00020-5.
[33] H. C. Müller-Redetzky, M. Felten, K. Hellwig, S.-M. Wienhold, J. Naujoks, B. Opitz, O. Kershaw, A. D. Gruber, N. Suttorp, and M. Witzenrath, "Increasing the inspiratory time and I:E ratio during mechanical ventilation aggravates ventilator-induced lung injury in mice," *Crit. Care*, vol. 19, no. 1, p. 23, Dec. 2015, doi: 10.1186/s13054-015-0759-2.
[34] Medicines and Healthcare Products Regulatory Agency. (2020). *Rapidly Manufactured Ventilator System (RMVS) Document RMVS001—Specification*. [Online]. Available: https://assets.publishing.service.gov.uk/government/uploads/system/uploads/attachment_data/file/879382/RMVS001_v4.pdf
[35] M. Alafeef and M. Fraiwan, "Smartphone-based respiratory rate estimation using photoplethysmographic imaging and discrete wavelet transform," *J. Ambient Intell. Humanized Comput.*, vol. 11, no. 2, pp. 693–703, Jun. 2019, doi: 10.1007/s12652-019-01339-6.
[36] A. Adami, R. Boostani, F. Marzbanrad, and P. H. Charlton, "A new framework to estimate breathing rate from electrocardiogram, photoplethysmogram, and blood pressure signals," *IEEE Access*, vol. 9, pp. 45832–45844, 2021, doi: 10.1109/ACCESS.2021.3066166.
[37] R. Lazazzera and G. Carrault, "Comparative study of different breathing rate estimation methods from PPG signals, on CAPNOBASE database," in *Proc. Comput. Cardiol. Conf. (CinC)*, Dec. 2020, pp. 1–4, doi: 10.22489/cinc.2020.064.
[38] I. Daubechies, *Ten Lectures on Wavelets*. Philadelphia, PA, USA: Society for Industrial and Applied Mathematics, Jan. 1992, doi: 10.1137/1.9781611970104.
[39] S. Li, S. Jiang, S. Jiang, J. Wu, W. Xiong, and S. Diao, "A hybrid wavelet-based method for the peak detection of photoplethysmography signals," *Comput. Math. Methods Med.*, vol. 2017, Nov. 2017, Art. no. e9468503, doi: 10.1155/2017/9468503.
[40] B. Hill and S. H. Annesley, "Monitoring respiratory rate in adults," *Brit. J. Nursing*, vol. 29, no. 1, pp. 12–16, Jan. 2020, doi: 10.12968/bjon.2020.29.1.12.
[41] N. Q. Al-Naggar, "Modelling and simulation of pressure controlled mechanical ventilation system," *J. Biomed. Sci. Eng.*, vol. 8, no. 10, pp. 707–716, 2015, doi: 10.4236/jbise.2015.810068.
[42] M. Williams, R. D. Porsolt, and P. Lacroix, "Safety pharmacology II-CV, GI, respiratory and renal safety," in *XPharm: The Comprehensive Pharmacology Reference*. Amsterdam, The Netherlands: Elsevier, 2007, pp. 1–22, doi: 10.1016/b978-008055232-3.63692-x.
[43] A. Özmen, E. Kropat, and G.-W. Weber, "Spline regression models for complex multi-modal regulatory networks," *Optim. Methods Softw.*, vol. 29, no. 3, pp. 515–534, Aug. 2013, doi: 10.1080/10556788.2013.821611.
[44] F. Yerlikaya-Özkurt, İ. Batmaz, and G. Weber, "A review and new contribution on conic multivariate adaptive regression splines (CMARS): A powerful tool for predictive data mining," in *Modeling, Dynamics, Optimization and Bioeconomics* (Springer Proceedings in Mathematics and Statistics). Switzerland: Springer, 2014, pp. 695–722, doi: 10.1007/978-3-319-04849-9_40.

NUZAT NUARY ALAM received the M.Sc. degree in bio-engineering: digital body from the University of Nottingham, U.K., in 2013. She is currently an Assistant Professor with American International University-Bangladesh (AIUB). Her research interests include new generation state-of-the-art electronics to develop medical devices and healthcare technologies.

RETHWAN FAIZ received the M.B.A. and M.Sc. degrees in electrical and electronic engineering from American International University-Bangladesh (AIUB), in 2014 and 2021, respectively. He is currently an Assistant Professor with AIUB. His research interests include wireless sensor networks, biomedical engineering, and nanoelectronics.

MD. SAYZAR RAHMAN AKASH received the B.Sc. degree in electrical and electronics engineering from American International University-Bangladesh (AIUB), Dhaka, Bangladesh, in 2022, where he is currently pursuing the M.Sc. degree in EEE. He joined the Center for Biomedical Research (CBR), Dr. Anwarul Abedin Institute of Innovation, AIUB, as a Research Assistant. His research interests include biomedical signal processing and analysis, healthcare systems, RF signal and antenna design, nanotechnology, robotics, automation and the IoT, and UAV applications.

TANVER SHIDDIQUE received the B.Sc. degree in electrical and electronics engineering from American International University-Bangladesh (AIUB), Dhaka, Bangladesh, in 2022. His research interests include biomedical signal processing and analysis, healthcare systems, automation and IoT, smart farming, and poultry management.

FAIRUZA FAIZ received the B.Sc. and M.Sc. degrees in electrical and electronics engineering from American International University-Bangladesh (AIUB), Dhaka, Bangladesh, in 2010 and 2014, respectively, and the Ph.D. degree in optical sensing from Victoria University, Melbourne, Australia, in 2020. Her research interests include optical sensors and photonic devices for the detection of physical parameters including environmental contaminants.

MOHAMMAD HASAN IMAM (Member, IEEE) received the Ph.D. degree in bio signal processing and modeling from The University of Melbourne, Australia, in 2015. He is currently an Associate Professor with the Department of Electrical and Electronic Engineering, American International University-Bangladesh (AIUB). His main research interests include bio-information processing, model-based system dynamics analysis, machine learning in healthcare, biomedical signal processing, and biomedical electronics.